DEVELOPMENT OF A FUEL CELL MODEL USING NATURAL GAS AS FUEL FOR SMALL ELECTRIC APPLIANCES APPLICATION

Penyarat Saisirirat*

Department of Mechanical Engineering Technology, College of Industrial Technology, King Mongkut's University of Technology North Bangkok, Bangkok, 10800, Thailand

Received 21 March 2017; Revised 21 July 2017; Accepted 27 July 2017

ABSTRACT

This work focuses on the fuel cell model using natural gas as fuel applied for small electric appliances. The solid oxide fuel cell (SOFC) is selected for this research because it can be operated with various kinds of fuels such as natural gas, carbon monoxide, methanol, ethanol and hydrocarbon compounds. In this study, a numerical model of an anode-supported SOFC with internal reforming of natural gas has been developed. The numerical model simultaneously solves mass, energy equations and chemical as well as electrochemical reactions. This model can predict the cell performance under the cell operating conditions. The cell performance is specified in the terms of cell voltage and power density at any specific current density. The power is limited for application to the small electric appliances. The influence of electrode microstructure on cell performance was also investigated. The results show that the cell performance almost insensitive to microstructure of cells unlike the operating conditions. The accuracy of the numerical model was validated by comparing with existing experimental results in available literatures.

KEYWORDS: *Cell performance; Electrode microstructure; Fuel Cell; Internal reforming; Natural gas; Numerical model; Small electric appliances*

* Corresponding authors; e-mail: penyarat@gmail.com,Tel: +668-9138-2120

INTRODUCTION

A fuel cell is a device that converts the chemical energy from a fuel into electricity through a chemical reaction of positively charged hydrogen ions with oxygen or another oxidizing agent. Fuel cells are different from batteries in requiring a continuous source of fuel and oxygen or air to sustain the chemical reaction, whereas in a battery the chemicals present in the battery react with each other to generate an electromotive force (emf) [1]. Fuel cells can produce electricity continuously for as long as these inputs are supplied. Fuel cells are used for primary and backup power for commercial, industrial and residential buildings and in remote or inaccessible areas. They are also used to power for small electric appliances, and also for vehicles. There are many types of fuel cells, but they all consist of an anode, a cathode, and an electrolyte that allows positively charged hydrogen ions (or protons) to move between the two sides of the fuel cell. The anode and cathode contain catalysts that cause the fuel to undergo oxidation reactions that generate positively charged hydrogen ions and electrons. The hydrogen ions are drawn through the electrolyte after the reaction. At the same time, electrons are drawn from the anode to the cathode through an external circuit, producing direct current electricity. At the cathode, hydrogen ions, electrons, and oxygen react to form water [1]. Fuel cells are typically classified by the type of electrolyte they use and by the difference in startup time ranging from 1 second for proton exchange membrane fuel cells (PEM fuel cells, or PEMFC) to 10 minutes for solid oxide fuel cells (SOFC). Solid oxide fuel cells (SOFCs) use a solid material, most commonly a ceramic material called yttria-stabilized zirconia (YSZ), as the electrolyte. They require high operating temperatures (600 –1000 °C) and can be run on a variety of fuels including natural gas [2].

In this work the focus is on the mathematical modelling of planar SOFC with direct internal reformation. The planar SOFC, provides high power density due to its shorter current flow path and lower ohmic polarization loss and simple to fabricate but the problems are the internal stress

and sealing due to non-uniform thermal expansion. To overcome problems, the operating temperature has been reduced to 600–800°C. Thinner electrolyte has been used to reduce ohmic loss. Anode-supported SOFC was considered due to its suitable configuration for direct internal reformation of hydrocarbon fuels that natural gas was used. The various models of gas transport inside the thick porous anode have been proposed by several researchers. Suwanwarangkul et al. [3] compared the accuracy to simulate gas transport phenomena inside anode of three different models: Fick's law model (FM), Stefan-Maxwell model (SMM) and Dusty-gas model (DGM). Among the three models, DGM provided the most accuracy to predict the gas transport behaviour inside anode. Ackmann et al. [4] applied the mean transport pore model (MTPM) to analyze mass transport in a two-dimensional and their model included the effect of chemical and electrochemical reactions on heat transfer inside the cell. Morel et al. [5] studied the direct internal reforming (DIR) process of methane within the thick porous anode of SOFC, based on the previously mentioned model but they taking into account mass transport along the gas channels and diffusion through the porous electrodes, as proposed by Ackmann [4]. Ho et al. [6] developed a numerical 3D model by using Star - CD. The model took into account detailed process including transport, chemical and electrochemical processes but their work does not considerinfluence of electrode microstructure and operating conditions.

In this study, the mathematical model which is used to predict the cell performance of a planar anode-supported SOFC when natural gas is the supplied fuel was developed. The effects of chemical and electrochemical reactions on the heat and mass transports insidethe cell were included in the model. The mass transport in gas flow channels is considered as mass convection, while the mass transport inside the porous electrode is considered as mass diffusion. The heat transfer model is included of convective heat transfer between solid and gas phase as well as conductive heat transfer in solid cell components. The endothermic heat consumed during steam-methane reforming and exothermic heat released from electrochemical reactions were included as heat sources.

MATERIALS AND METHODS

Mathematical Modeling

Model assumptions and cell geometry

The supplied natural gas to the anode was assumed to have the following compositions: 87% by mole of CH_4, 6% by mole of C_2H_6 and 2% by mole of higher hydrocarbon with 30% pre-reformation following the suggestion by Meusinger et al [7] to prevent excessive temperature gradient across the cell. Air supplied to cathode was use as oxidant. All gases behave as ideal gases. The electrode is homogeneous. Mass transport in porous electrode is considered as mass diffusion companied by chemical and electrochemical reactions. Steam reforming reaction is assumed to occur at the surface of anode and water gas shifted reaction is assumed to occur inside the void volume of anode. The electrochemical reaction occurs at the vicinity area of anode and electrolyte interface. A schematic one dimension model of a co-flow planar anode-supported SOFC is shown in Fig.1. The dimension of cell components and standard parameters used in calculation are given in Table1.

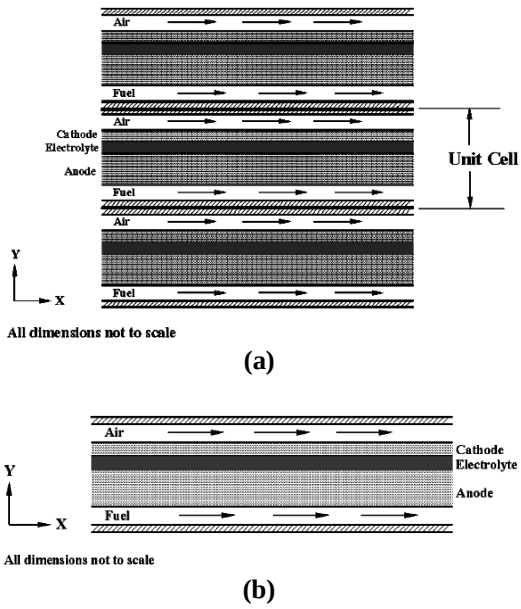

Fig. 1 A schematic model of a planar anode - supported SOFC (a) Stack schematic; (b) 1 cell schematic used in the modeling.

Table 1 Standard parameters used in this study

Parameters	Values
Anode thickness	2 mm
Anode length	10 cm
Anode porosity (ε)	0.4
Anode tortuosity (τ)	2.75
Anode pore radius (r_{an})	1 μm
Cathode thickness	60 μm
Cathode length	10 cm
Cathode porosity (ε)	0.4
Cathode tortuosity (τ)	2.75
Cathode pore radius (r_{cat})	1 μm
Electrolyte thickness	60 μm
Electrolyte length	10 cm
Transfer coefficient (α)	0.5
Cathode exchange current density (j_{oc})	$0.1*10^4$[A m^{-2}]
Anode exchange current density (j_{oa})	$1*10^4$ [A m^{-2}]
Cathode limiting current density ($j_{lim,c}$)	$1*10^5$ [A m^{-2}]
Electrolyte constant (A)	$9*10^7$ [K ohm*m^{-1}]
Electrolyte activation energy (G_{act})	$100*10^3$ [J mol^{-1}]
Faraday constant (F)	96485 [C mol^{-1}]
Specific surface area (A_S)	$3*10^6$ [m^2 m^{-3}]
Anode effective thermal conductivity ($\lambda_{eff,an}$)	3 [W m^{-1} K^{-1}]
Anode convective heat transfer coefficient (h_{an})	57 [W m^{-2} K^{-1}]
Cathode effective thermal conductivity ($\lambda_{eff,an}$)	3.8 [W m^{-1} K^{-1}]
Cathode convective heat transfer coefficient (h_{an})	49 [W m^{-2} K^{-1}]
Electrolyte effective thermal conductivity ($\lambda_{eff,an}$)	1.8 [W m^{-1} K^{-1}]
Fuel flow rate	$0.5*10^{-3}$ [m^3 min^{-1}]
Air flow rate	$5*10^{-3}$ [m^3 min^{-1}]
Operating pressure (P)	1 atm
Operating temperature (T)	800 °C

Mass transport

Mass transport in SOFC composed of 2 parts, mass diffusion in porous electrodes and mass convection in gas flow channels. The cathode is relatively thin comparable to the anode thickness, the mass diffusion in the cathode side could be omitted in this computation.

Mass balance in porous anode

The gas transport within the anode pores, which is strongly dependent on the anode microstructure, can be described by combining the Stefan-Maxwell and Knudsen diffusion relations. Mass diffusive flux deduced as Eq.1.

$$\frac{N_i}{D_{i,k}^{eff}} + \sum_{j=1,j\neq i}^{n} \frac{y_j N_i - y_i N_j}{D_{ij}^{eff}} = -\frac{P}{RT}\left(\frac{dy_i}{dy}\right) \quad (1)$$

where y_i is mole fraction, while N_i and N_j are the molar flux of species i and j. $D_{i,k}^{eff}$ is the effective Knudsen diffusion coefficient and D_{ij}^{eff} is the effective diffusion coefficient.

$$D_{ij}^{eff} = \psi D_{ij} \quad or \quad D_{ij}^{eff} = (\varepsilon^{1.5})D_{ij} \quad (2)$$

$$D_{i,k}^{eff} = \psi D_{i,k} \;\; ; \quad D_{i,k} = (2/3)\bar{r}\sqrt{(8RT/\pi M_i)} \quad (3)$$

ψ is the ratio between porosity and tortousity and M_i is molecular weight of species i. The mass balance of all species i in the porous anode where both mass diffusion and chemical reactions occur is

$$\frac{\psi}{RT}\frac{d(y_i P)}{dt} = -\nabla \cdot N_i + r_i \quad (4)$$

Two types of chemical reactionsoccur at anode during supplying the fuel cells with natural gas. The reaction rate of methane-steam reformingand water gas shiftedcan be determined from Arhenius ' curve fits of the data reported in the reference [5]. The molar species formation rate, r_i in Eq.(4) can be calculated from Eqs.(5)–(9). The minus sigh refers to the consuming rate of each species, while the plus refers to the production rate.

$$r_{CH_4} = -R_1 \quad [\text{mol m}^{-3}\text{s}^{-1}] \quad (5)$$

$$r_{H_2O} = -R_1 - R_2 \quad [\text{mol m}^{-3}\text{s}^{-1}] \quad (6)$$

$$r_{CO} = R_1 - R_2 \quad [\text{mol m}^{-3}\text{s}^{-1}] \quad (7)$$

$$r_{H_2} = 3R_1 + R_2 \quad [\text{mol m}^{-3}\text{s}^{-1}] \quad (8)$$

$$r_{CO_2} = R_2 \quad [\text{mol m}^{-3}\text{s}^{-1}] \quad (9)$$

The current density from electrochemical reaction of hydrogen can be calculated by Faraday's law.

$$N_{H_2} = j/(2 \cdot F) \quad (10)$$

$$N_{H_2O} = -j/(2 \cdot F) \quad (11)$$

Mass balance in gas flow channels

For steady state, mass balance for each species i can be deduced as in Eq. (12).

$$\frac{dF_i}{dx} = 2\pi X \nu_i N_{i(y=0)} \quad (12)$$

where F_i is molar flow rate for species i and v_i is stoichiometric coefficient (–1 for reactant, +1 for product).

Heat transfer within the cell

The heat transfer in porous electrodes and dense electrolyte is dominated by conduction,

$$\lambda^{eff}\left(\frac{\partial^2 T}{\partial x^2}+\frac{\partial^2 T}{\partial y^2}\right)+q=0 \quad (13)$$

where q is heat source term. Heat consumed during methane-steam reformation at the surface of anode is $q_1 = R_1 \cdot A_s \cdot (-\Delta H_1)$ and heat released during the water - gas shifted reaction in the void volume of anode is $q_2 = R_2 \cdot \varepsilon \cdot (-\Delta H_2)$. Heat release from the electrochemical reaction at the electrode-electrolyte interface is $q_3(x) = \frac{j(x)}{2F}\Delta H_{H_2O} + j(x)\cdot V_c$, A_S is specific surface area, ε is porosity and ΔH is enthalpy of formation. Heat convection at interface between gas flow channels and electrode is.

$$q_{conv,i} = h_i(T_i - \overline{T}_{c,i}) \quad (14)$$

Cell electrical performance

Cell voltage V_C is assumed constant along cell length and can be calculated by potential balance,

$$V_C = E_{j=0} - (\eta_{ohmic} + \eta_{conc,a} + \eta_{conc,c} + \eta_{act,a} + \eta_{act,c}) \quad (15)$$

where $E_{j=0}$ is the open circuit voltage and can be calculated from Nernst' s equation,

$$E = E^\circ + (RT/4F)\ln\left(\left(p^c_{O_2}\left(p^a_{H_2}\right)^2\right)\Big/\left(p^a_{H_2O}\right)^2\right) \quad (16)$$

E° is standard Nernst potential at 1 atm and 25°C. $p^a_{H_2O}$ is water partial pressure, $p^a_{H_2}$ and $p^a_{O_2}$ are hydrogen and oxygen partial pressure. The parameter η_{ohmic} is ohmic polarization, in anode and cathode are assumed to be negligible, hence the ohmic polarization is only related to the electrolyte resistance. η_{conc} is the concentration polarization and η_{act} is the activation polarization. Therefore ohmic polarization based on electrolyte resistance can be determined from (17).

$$\eta_{ohmic} = j(t^E/\sigma) \quad (17)$$

where t^E is thickness of electrolyte. σ is electrolyte conductivity. The anodic and cathodic concentration can be seen as in eq. (18) and (19).

$$\eta_{conc,a} = (RT/2F)\ln((y_{H_2}y^\circ_{H_2O})/(y^\circ_{H_2}y_{H_2O})) \quad (18)$$

$$\eta_{conc,c} = (RT/2F)\ln(1-(j/j_{lim,c})) \quad (19)$$

where y_i and y°_i is mole fraction at nonzero and zero current densities at anode-electrolyte interface. $j_{lim,c}$ is cathode limiting current density. The activation polarization terms relate to electrochemical reaction located at electrode-electrolyte interface which are expressed as eqs. 20–21. $j_{o,a}$, $j_{o,c}$ are anodic, cathodic current densities at overvoltage begins to move from zero.

$$\eta_{act,a} = (RT/F)\,arcsinh(j/(2\cdot j_{o,a})) \quad (20)$$

$$\eta_{act,c} = (RT/F)\,arcsinh(j/(2\cdot j_{o,a})) \quad (21)$$

The Runge-Kutta method was used to solve mass diffusion equations coupled with heat transfer equations. The molar fraction of species i at $y_{i(x,\,y=0)}$ is equal to the molar fraction in the gas flow channels. At y equal to anode thickness t^A, the mass flux N_i is zero for CH_4, CO and CO_2, while N_i is given by the Faraday's law for H_2 and H_2O. The numerical iteration is repeated until the predicted current density agrees with corresponding current density to the specified cell voltage (V_C) in eq. 15.

RESULTS AND DISCUSSION

The developed model can be used to investigate the effects of operating conditions and design parameters, especially the geometry of electrode microstructure on the performance of a planar anode supported SOFC. First, simulations have been performed on the basis of standard physical parameters shown in Table 1. Operating conditions have been set to 800 °C for the gas temperature, 1 atm for the gas-phase pressure, 100 $mLmin^{-1}$ for both the anodic reactant and the cathodic (with 21% O_2) flow rates. According to literature [5], an S/C ratio equal to 1 allows the avoidance of carbon deposition at 800 °C. Effects of individual parameter on cell performance are studied. The effect of operating temperature on the cell's current density and voltage is shown in Fig. 2.

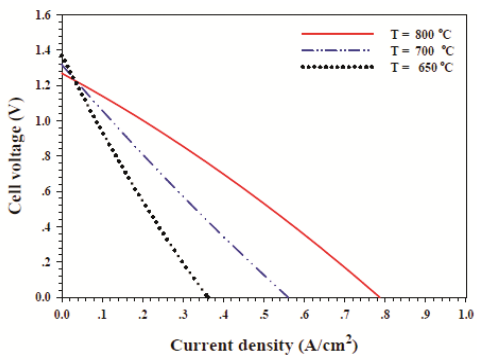

(a)

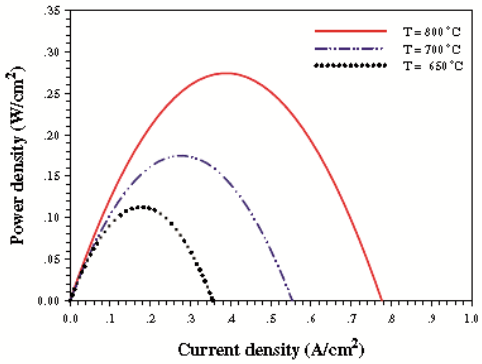

(b)

Fig. 2 (a) Effect of temperature on cell voltage; (b) Effect of temperature on cell power density.

Figure 2(a) shows that, at zero current density, the open circuit voltage decreases as temperature increases, whereas when the current density increases, the cell voltage increases with the operating temperature of the cell. Increase in operating temperature not only enhances the rate of electrochemical reaction, but also increases the rate of ionic conductivity, which in turn minimizing the ohmic contribution to the cell overpotential and thus enhancing the cell voltage and cell power density as shown in Fig. 2(a) and 2(b) respectively. The mathematicalmodel predicted that the maximum power density of the cell, about 0.28 W cm^{-2}, is given at current density of 0.38 A cm^{-2} and cell voltage of 0.73 V when the cell is operated at the standard pressure of 1 atm and temperature of 800 °C, with the fuel utilization of 48%. Fig. 3(a) and (b) show the effects of operating pressure on the cell voltage and on power density at the specified current density, respectively. Both cell voltage and power density increase with the operating pressure due to the increase in reactant concentration.

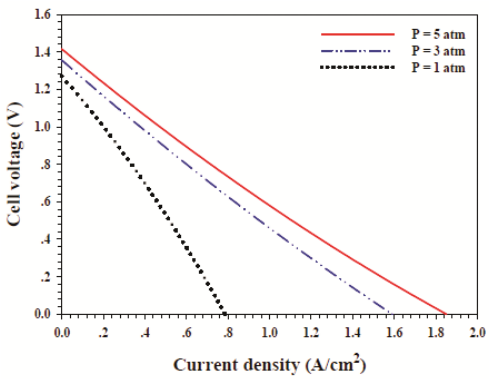

(a)

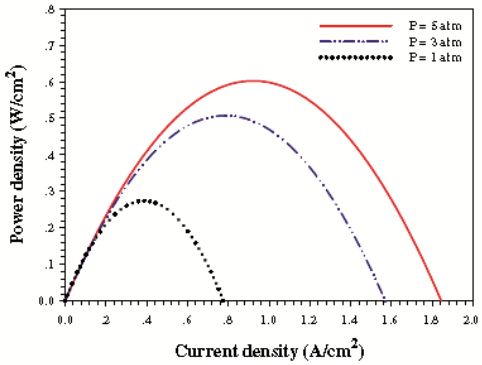

(b)

Fig. 3 (a) Effect of pressure on cell voltage; (b) Effect of pressure on cell power density.

It can be observed that increasing the pressure not only increases the open circuit voltage but also increases the actual cell voltage. With the increase of pressure, the reactant concentrationat the reaction sites increases. This in turn enhances the rate of electrochemical reaction and rate of mass transport, resulting in the minimization of anode and cathode overpotentials and hence producing better performance. However, increasing the operating pressure results in other problems such as limitations on material selection, gas sealing, and mechanical strength of the planar SOFC cellcomponents [1].

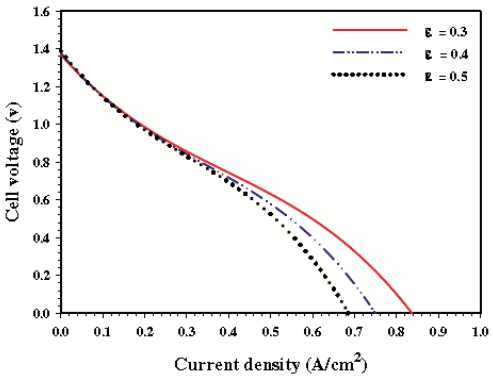

(a)

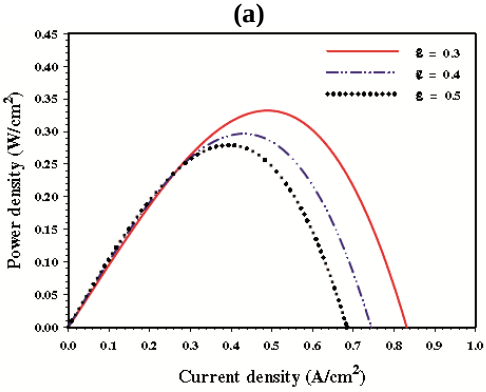

(b)

Fig. 4 (a) Effect of porosity on cell voltage; (b) Effect of porosity on cell power density.

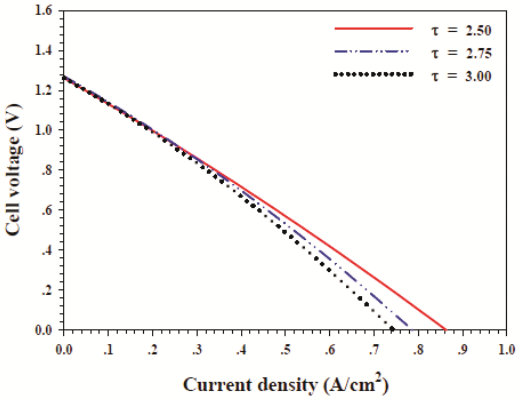

(a)

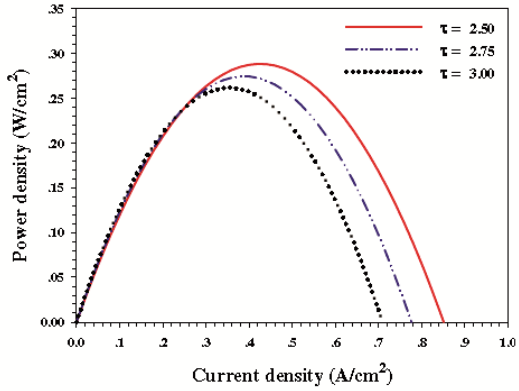

(b)

Fig. 5 (a) Effect of tortuosity on cell voltage; (b) Effect of tortuosity on cell power density.

In order to study the effects of cell geometry such asporosity, tortuosityand electrolyte thickness oncell performance, the operating condition is set at 800 °C and 1 atm. The effects of porosity on cell voltage and onpower density at the specified current density are shown in Figures 4(a) and 4(b). The cell voltage and power density only decrease with the porosity at high current density. Increasing the porosity of the cell components decreases the cell performance. Increasing the porosity increases the void fraction and decreases the solid fraction of the porous medium resulting in the reduction of the active surface area available for the electrochemical reaction. Moreover, the effective ionic and electron conductivities of the porous decrease with the increase of porosity, which results in the increase of ohmic overpotential. Although the concentration overpotential decreases with the increase of porosity due to the increased mass transport rates; the cell voltage and power density decreases due to increasing of ohmic overpotential with porosity. The effects of tortuosity on the cell performance are reported in Fig. 5(a) and 5(b). Increasing the tortuosity of the porous medium decreases the performance of the cell. Increasing the tortuosity means that increasing the length of tortuous flow paths, which leads to additional resistance to the reactant species diffusing through the porous medium, thus resulting in the reduction of reactant concentration at the reaction sites and thereby decreasing the rate of electrochemical reaction. In addition, the effective ionic and electronic conductivities decrease with the increase of tortuosity, resulting in the increase of ohmic overpotential, and hence decreasing cell voltage and power density.

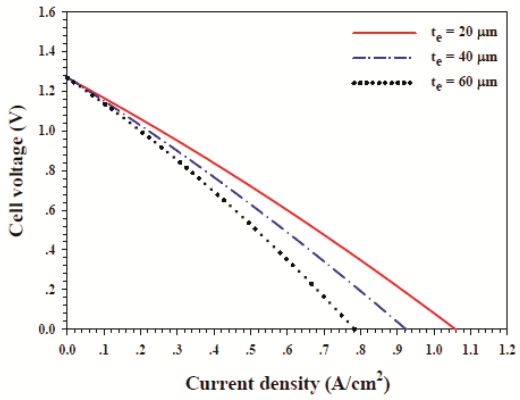

(a)

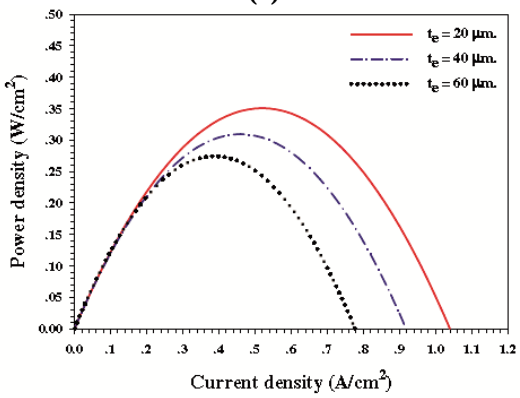

(b)

Fig. 6 (a) Effect of electrolyte thickness on cell voltage; (b) Effect of electrolyte thickness on cell power density.

Figures 6(a) and 6(b) show the effects of electrolyte thickness on cell performance. The cell voltage and power density at a specified current density increase as the electrolyte thickness decreases due to the decrease of ohmic loss.

CONCLUSION

A mathematical model for predicting the performance of a co-flow planar anode supported solid oxide fuel cell with internal reforming of natural gas has been developed. The model simultaneously solved mass and energy transport equations as well as chemical and electrochemical reactions. The model can effectively predict the cell performance at various operating conditions. The model is useful in analyzing the effects of electrode microstructure such as porosity and tortuosity as well as electrolyte thickness on cell performance. The performance of the cell was reported in terms of cell voltage and power density at specified current densities. Regarding the temperature effect, as the operating temperature increases, the concentration overpotential will increase, while both the ohmic and activation overpotentials will decrease drastically. The overall effect will be a significant increase in cell voltage and power density. Moreover, the cell voltage and power density can be increased by increasing the operating pressure to reduce both the concentration and activation overpotentials. The simulation results show that the steady state performance is almost insensitive to microstructure of cells such as porosity and tortuosity unlike the operating pressure and temperature. The power output could be maximized by adjusting porosity and tortuosity to an optimal value. At standard operating pressure (1 atm) and 800 °C with 48% fuel utilization, an output cell voltage of 0.73 V, a current density of 0.38 A cm^{-2} with a power density of 0.28 W cm^{-2} was predicted. The model predicted results are validated with the experimental data found in the literature. A good agreement is obtained between the predicted values and the measured data.

ACKNOWLEDGEMENTS

Authors would like to acknowledge with gratitude the financial support from the College of Industrial Technology, King Mongkut's University of Technology North Bangkok.

REFERENCES

[1] J. Larminie, A. Dicks, Fuel Cell Systems Explained, second ed., John Wiley and Sons, West Sussex, England, 2003.

[2] S.C. Singhal, K. Kendal, High Temperature Solid Oxide Fuel Cells:Fundamentals Design and Applications, first ed., Elsevier Science, 2003.

[3] R. Suwanwarangkul, E. Croiset, M.W. Fowler, P.L. Douglas, E. Entchev, M.A. Douglas, Performance comparison of Fick's, Dusty-Gas and Stafan-Maxwell models to predict the concentration overpotential of a sofc anode, J. Power Sources. 122 (2003) 9–18.

[4] T. Ackmann, L.G.J. De Haart, W. Lehnert, D. Stolten, Modeling of mass and heat transport in planar substrate type sofcs, J. Electrochem. Soc. 150(6) (2003) A783–A789.

[5] B. Morel, J. Laurencin, Y. Bultel, F. Lefebvre-Joud, Anode-supported sofc model centered on the direct internal reforming, J. Electrochem. Soc. 152(7) (2005) A1382–A1389.

[6] T.X. Ho, P. Kosinski, A.C. Hoffmann, A. Vik, Effects of heat sources on the performance of a planar solid oxide fuel cell. Int. J. Hydrogen Energy. 35(9) (2010) 4276–4284.

[7] J. Meusinger, E. Riensche, U. Stimming, Reforming of natural gas in solid oxide fuel cell systems. J. Power Sources. 71 (1998) 315–320.